J Mater Sci: Mater Electron (2017) 28:6977–6981
DOI 10.1007/s10854-016-5864-8

Light emitting mechanisms dependent on stoichiometry of Si-rich-SiN_x films grown by PECVD

T. V. Torchynska[1] · J. L. Casas Espinola[1] · J. A. Jaramillo Gomez[2] · J. A. Bentosa Gutiérrez[2] · L. Khomenkova[3] · A. Slaoui[4]

Received: 8 August 2016 / Accepted: 8 October 2016 / Published online: 22 October 2016
© Springer Science+Business Media New York 2016

Abstract Light emission and morphology of silicon-rich silicon nitride films grown by plasma-enhanced chemical vapor deposition were investigated versus film's stoichiometry. The excess silicon content in the films was controlled varying the NH_3/SiH_4 gas flow ratio from 0.45 up to 1.0. High-temperature annealing was employed to form the silicon quantum dots (QDs) and to enhance the photoluminescence (PL) in visible spectral range. The PL spectrum was found to be complex. The competition of five PL bands leads to the non-monotonous variation of total PL peak position in the range of 1.55–2.95 eV when the Si excess content increases. The shape of PL spectra depends also on an excitation light wavelength. It is shown that for the films fabricated with $R \leq 0.56$ and $R \geq 0.67$ the dominant contribution into PL spectra is given by native SiN_x defects, whereas in the films obtained with $R = 0.59$–0.67 the Si-QDs form the main radiative channel. The highest PL intensity is detected in Si-rich SiN_x films grown at $R = 0.59$–0.67 as well. PL mechanisms are discussed in terms of the contribution of different radiative channels in the light emission process that can show the ways for the optimization of SiN_x light-emitting properties.

✉ T. V. Torchynska
ttorch@esfm.ipn.mx

[1] Instituto Politécnico Nacional, ESFM, 07738 Mexico, DF, Mexico

[2] Instituto Politécnico Nacional, UPIITA, 07320 Mexico, DF, Mexico

[3] V. Lashkaryov Institute of Semiconductor Physics at NASU, Kiev, Ukraine

[4] ICube, 23 rue du Loess, BP 20 CR, 67037 Strasbourg Cedex 2, France

1 Introduction

Bandgap engineering the Si-based material via control of the distribution of Si quantum dots (QDs) in silicon nitride (SiN_x) matrix offers future applications of Si-based nanostructures in optoelectronics, as low-cost, miniaturized, and CMOS-compatible light-emitting diodes, solar cells and photovoltaic devices [1–4]. Additionally, SiN_x films demonstrate a high density of deep defects [5, 6] and bright luminescence in UV–visible spectral ranges [7, 8]. In the past, the main attention was concentrated on developing the luminescent Si-QDs embedded in a SiO_2 matrix [9–11]. However, the SiO_2 insulating character remains a barrier for the production of electrically pumped light-emitting diodes or photovoltaic cells. Si-QDs in a silicon nitride offer several advantages due to the structural stability at technological processing and better electrical properties owing to lower tunneling barriers [12]. The last aspect making SiN_x films suited for electroluminescent devices [12].

In addition, Si-QDs in silicon oxide are subject to charge trapping at the Si/SiO_2 interface that limits the emission quanta from Si-QDs to less than 2 eV [13]. Si-QDs coordinated with nitrogen atoms, as expected, do not exhibit such limitation that permits emission obtaining with the quant energy across the whole visible spectral range [14, 15]. Bright emission from Si-rich-silicon nitride films grown by the plasma enhanced chemical vapor deposition (PECVD) was reported early in [12, 14–18]. Some authors attributed this photoluminescence (PL) to exciton recombination inside of Si-QDs [12, 14, 15]. In contrary, other authors assigned emission to the recombination via native defects or dangling bonds in SiN_x [18, 19]. In addition, the SiN_x emission was escribed also to the electron–hole recombination via band-tails in amorphous SiN_x matrix

[20, 21] or to light interference in thick SiN_x films [22]. Thus the nature of radiative optical transitions in silicon nitride films with Si-QDs is still debatable.

In this work, the morphology and emission of Si-rich-silicon nitride films grown by PECVD were investigated versus excess silicon contents. PL is studied within the temperature range 20–300 K using different excitation light wavelengths, UV (325 nm) or visible (488 and 532 nm), that permits getting insight in the nature of optical transitions.

2 Experimental details

Si-rich SiN_x films were grown by PECVD on p-type Si (100) substrates. The stoichiometry of films was changed by varying the NH_3/SiH_4 (99.9999 %) gas flow ratio (R) in the range of 0.45–1.0. The pressure, plasma power and film growth temperature were 0.5 Torr, 20 W, and 350 °C, respectively. Annealing at 1100 °C for 30 min in nitrogen flow was used to obtain the Si-QDs in SiN_x films.

Si-rich SiN_x films were investigated by means of atomic force microscope (AFM) and photoluminescence methods. PL spectra were excited by a 325-nm (3.82 eV) line of a He–Cd laser, or by a 488-nm (2.54 eV) line of an Ar+ laser, or by a 532-nm (2.33 eV) line of a solid state laser. The power of excitation beam was about 80 mW. The details of PL experiments can be found in [23, 24]. PL spectra were measured in the temperature range of 20–300 K using a closed-cycle He cryostat. Atomic force microscope (AFM) study of sample's surface was performed using a Nano-Scope IIIa tool operated in tapping and covered modes.

3 Results and discussion

AFM images of SiN_x films grown at different R parameters are shown in Fig. 1. The roughness in films varies versus R: decreases from 14.9 nm (at R = 1.0) down to 13.4 nm (at R = 0.83), 9.5 nm (at R = 0.67) and 7.8 nm (at R = 0.50). It was shown early at the X-ray diffraction

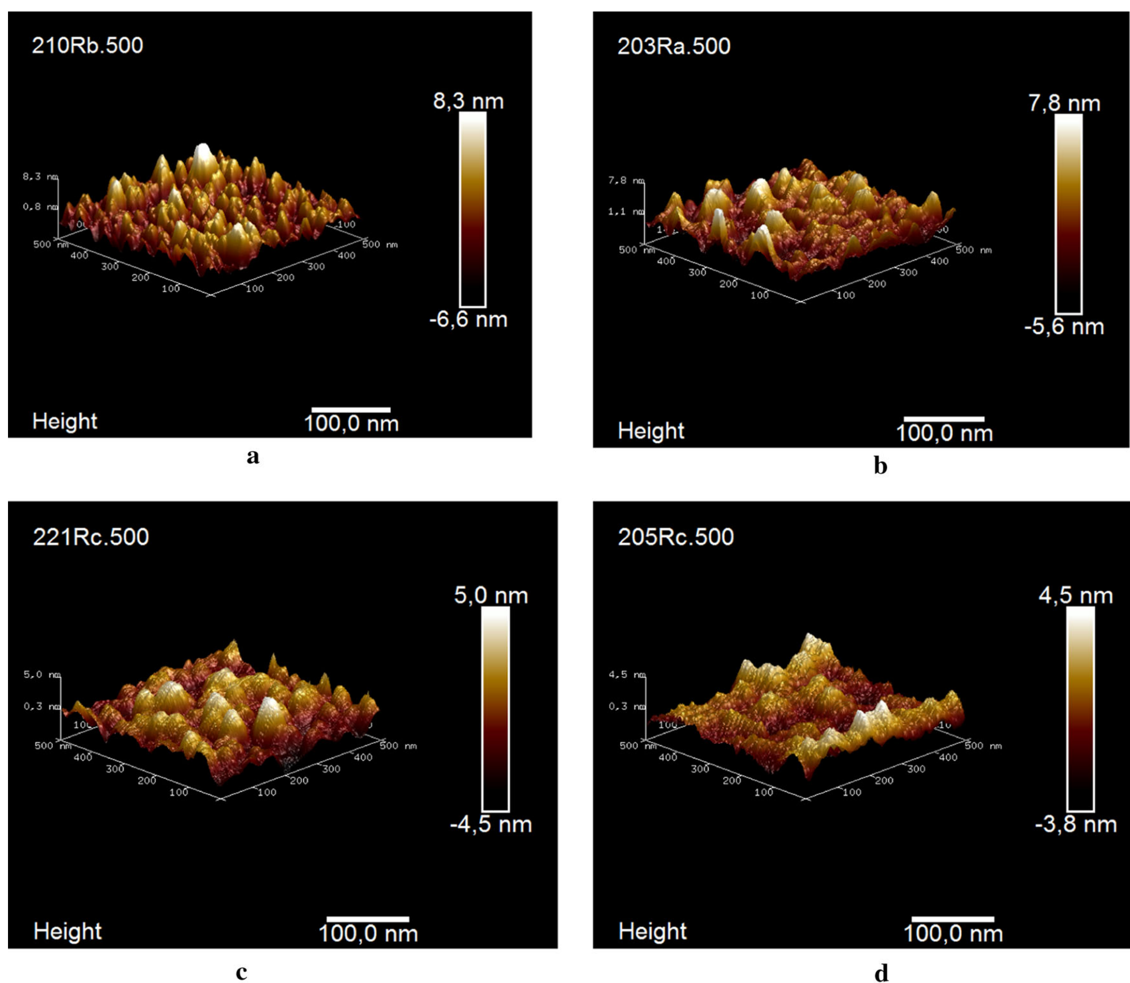

Fig. 1 AFM images of SiN_x films grown at different R parameters: **a** R = 1.0, **b** R = 0.83, **c** R = 0.67, **d** R = 0.50

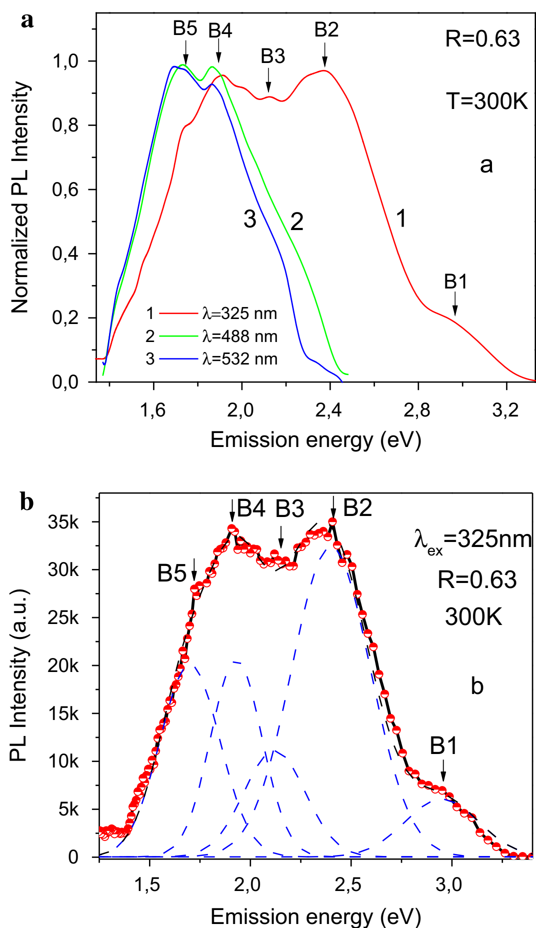

Fig. 2 PL spectra **a** of the film grown at R = 0.63 measured at 300 K using different excitation light wavelengths: 325 nm (*1*), 488 nm (*2*), 532 nm (*3*). The deconvolution example **b** of the PL spectrum 1 from **a** on the five Gaussian shape PL bands

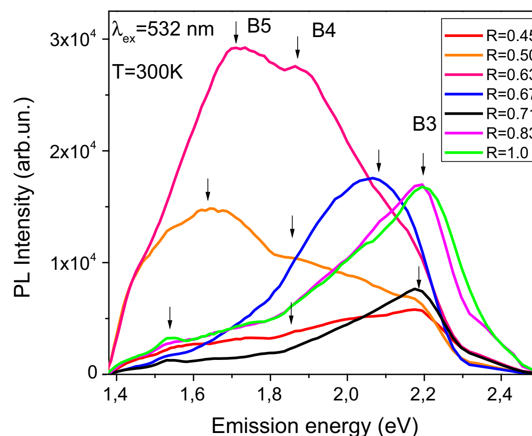

Fig. 3 PL spectra measured at 300 K at excitation light wavelength of 532 nm of the SiN_x films grown at different R parameters indicated in Fig. 3

study [18] that the SiN_x matrix had the hexagonal Si_3N_4 phase in the films obtained at R = 0.7–1.0 with the sizes of Si_3N_4 nanocrystals (NCs) of 26–30 nm. The Si_3N_4 NC size falls down to 2.8–3.0 nm at R = 0.63–0.67 and the SiN_x films became amorphous at R = 0.45–0.50 [18]. Thus, the change of roughness can be related to changing the crystallinity of SiN_x matrix versus R parameters [18].

PL spectra of annealed films at 300 K demonstrate the variation of the shape with excitation light energy (Fig. 2a). The broader PL spectrum is observed at higher excitation energy (3.82 eV) demonstrating the superposition of several PL bands. All PL spectra excited by 3.82-eV light can be decomposed on five PL bands (Fig. 2b) with the maxima at 2.95 eV (B1), 2.45 eV (B2), 2.20 eV (B3), 1.92 eV (B4) and 1.72 eV (B5). The former two PL bands are well known in Si-rich-SiN_x films [25–27]. Two paramagnetic defects were detected early in SiN_x matrix by the electron spin resonance method: the K center—Si atom with one Si dangling bond (emission at ~2.40–2.50 eV) and the N center—N atom with one N dangling bond ($N_4^+ \rightarrow E_v$ and $E_c \rightarrow N_2^0$, emission at ~2.9–3.1 eV) [27]. In addition, the PL band with the peak at 590 nm (2.1 eV) was assigned early to oxygen related defects in silicon nitride [28].

Thus, the PL bands B1 and B2 using mentioned above defect models can be assigned to the recombination via native defects in the SiN_x matrix: N and Si dangling bonds, respectively. The PL band B3, apparently, is connected with oxygen related defects in SiN_x [28]. To avoid the high energy emission of SiN_x related defects, the PL spectra have been detected using low energy excitation light (Fig. 2a) with the wavelengths 488 nm (2.54 eV) or 532 nm (2.33 eV) that permit to study two other PL bands: B4 and B5.

In Fig. 3 the PL spectra of SiN_x films grown at different R and excited by the 532 nm light have been shown. The main band in PL spectra of films obtained at R = 0.71–1.0 is 2.20 eV PL band (B3). PL spectra shift to low energy spectral range with increasing the Si contents in SiN_x films (decreasing R) and the PL bands B4 and B5 appear at $R \leq 0.67$ (Fig. 3). Si content increasing leads to Si-QD size raising that has to be accompanied by a low energy shift of the PL band related to exciton emission in Si-QDs. Actually, as it is clear from Fig. 3, the peak position of the PL band B5 changes monotonically versus excess Si contents from 2.09 eV (R = 0.67) down to 1.71 eV (R = 0.63) then to 1.63 eV (R = 0.50) and to 1.56 eV (R = 0.45). This fact permits to assign the PL band B5 to exciton emission in Si-QDs [9].

The PL band B4 appears synchronously with the PL band B5 (Fig. 3) and both these PL bands overlapped very much at low Si excess contents (R = 0.63–0.71). PL intensities of bands B4 and B5 increase essentially in the film grown at R = 0.63 and then decreasing monotonically

in the films grown at R = 0.45–0.50. This synchronous behavior can be connected with the close location of emitting centers B4 to Si-QDs that allows the energy exchange between them. It is clear from Fig. 3 as well that the peak of PL band B4 does not change with increasing the Si content in SiN_x films (R = 0.67 down to 0.45). Note, that the center responsible for the PL band B4 can be located at the Si-QDs/SiN_x interface and, probably, related to N dangling bonds as well. In this case, the optical transition between $N_4{}^+$ and N_2^0 energy levels proposed early in [25] for the orange PL band in SiN_x looks completely reliable for the PL band B4.

PL intensity increasing in the films obtained with $R \leq 0.67$ (Fig. 3) is connected with the fact that for this SiN_x composition the excitation light used (2.33 eV) becomes higher or equal to the SiN_x bang gap [29]. PL intensity decreasing in the films grown with R = 0.45–0.50 is related, apparently, to the efficient carrier nonradiative recombination in amorphous SiN_x and Si phases. The last one was detected early in Si rich SiN_x films with high Si excess even after high temperature annealing [18].

To confirm that the PL band B5 is owing to exciton emission in Si-QDs, PL spectra have been studied at different temperatures within the range 20–300 K (Fig. 4). As one can see in Fig. 4, the PL peaks of bands B3 and B4 do not change their positions versus temperatures. This behavior is typical for the carrier radiative recombination

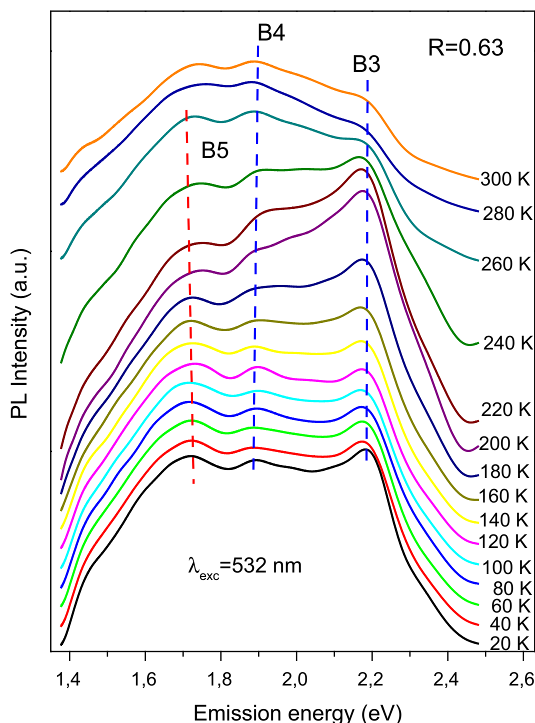

Fig. 4 PL spectrum evolution in the film grown at R = 0.63 with temperature of measurement in the range of 20–300 K. Excitation energy is 2.33 eV (532 nm)

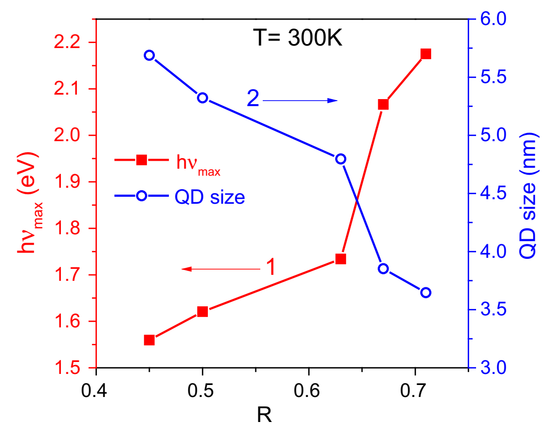

Fig. 5 The variation of PL peak positions (*1*) for exciton emission in Si-QDs and QD sizes (*2*) versus R parameters

via native defects in the SiN_x matrix. Simultaneously, the PL peak B5 shifts to lower energy from 1.73 eV (20 K) down to 1.69 eV (300 K) and varies on 40 meV that is very close to the shrinkage of the bulk Si band gap (45 meV) versus temperatures in the range 20–300 K [30]. Thus, we can conclude again that PL band B5 is connected with exciton emission in Si-QDs.

The size of Si-QDs in different SiN_x films can be estimated using formula $E = 1.13 + 13.9/d^2$ proposed early in [31] for Si band-gap increasing at QD size decreasing. Figure 5 presents the variation of PL peaks of the band B5 and Si QD sizes in studied films versus parameter R. The estimation has shown that the Si-QD size varies from 5.7 nm in films obtained at R = 0.45 to 3.6 nm in films grown with R = 0.71.

4 Conclusions

The variations of excitation light energies and temperatures at the PL spectrum measurement allow detecting the different radiative channels in the Si rich SiN_x films with the different stoichiometry. It is shown that for the films fabricated with $R \leq 0.56$ and $R \geq 0.67$ the main contribution into PL spectra is given by the native SiN_x defects, whereas in the films obtained at R = 0.59–0.67 the Si-QDs form the main radiative channel. The highest PL intensity is detected in Si-rich SiN_x films grown at R = 0.59–0.67 as well that permits to consider this range of R as optimized for the bright emission of Si-rich SiN_x films.

Acknowledgments The authors thank the Secretary of Investigation and Postgraduate Study of National Polytechnic Institute (SIP-IPN) of Mexico (Project 20160285), National Council of Science and Technology (CONACYT) of Mexico (Project 258224), the National Academy of Sciences of Ukraine and Center of National Scientific Research (CNRS) of France for the financial supports.

References

1. C. Bonafos, M. Carrada, G. Benassayag, S. Schamm-Chardon, J. Groenen, V. Paillard, B. Pecassou, A. Claverie, P. Dimitrakis, E. Kapetanakis, V. Ioannou-Sougleridis, P. Normand, B. Sahu, A. Slaoui, Mater. Sci. Semicond. Process **15**, 615 (2012)
2. M.S. Yang, K.S. Cho, J.H. Jhe, S.Y. Seo, J.H. Shin, K.J. Kim, D.W. Moon, Appl. Phys. Lett. **85**, 3408 (2004)
3. G.-R. Lin, Y.-H. Pai, Ch-T Lin, Ch-Ch. Chen, Appl. Phys. Lett. **96**, 263514 (2010)
4. Ch-D Lin, Ch-H Cheng, Y.-H. Lin, Ch-L Wu, Y.-H. Pai, G.-R. Lin, Appl. Phys. Lett. **99**, 243501 (2011)
5. J. Carreras, J. Arbiol, B. Garrido, C. Bonafos, J. Monserrat, Appl. Phys. Lett. **92**, 091103 (2008)
6. B.S. Sahu, F. Delachat, A. Slaoui, M. Carrada, G. Ferblantier, D. Muller, Nanoscale Res. Lett. **6**, 178 (2011)
7. C. Liu, C. Li, A. Ji, L. Ma, Y. Wang, Z. Cao, Nanotechnology **16**, 940 (2005)
8. Z. Pei, Y.R. Chang, H.L. Wang, Appl. Phys. Lett. **80**, 2839 (2002)
9. T.V. Torchynska, in *Nanocrystals and Quantum Dots of Group IV Semiconductors*, ed. by T.V. Torchynska, Y. Vorobiev (American Scientific Publisher, Stevenson Ranch, 2010), pp. 42–84
10. A. Meldrum, A. Hryciw, A.N. Mac Donald, C. Blois, T. Clement, R. De Corby, J. Wang, Quan Li, J. Lumin. **121**, 199 (2006)
11. U. Kahler, H. Hofmeister, Opt. Mater. **17**, 83 (2001)
12. G.Y. Sung, N.M. Park, J.H. Shin, K.H. Kim, T.Y. Kim, K.S. Cho, C. Huh, IEEE J. Sel. Top. Quantum. Electron. **12**, 1545 (2006)
13. M.V. Wolkin, J. Jorne, P.M. Fauchet, G. Allan, C. Delerue, Phys. Rev. Lett. **82**, 197 (1999)
14. N.M. Park, C.J. Choi, T.Y. Seong, S.J. Park, Phys. Rev. Lett. **86**, 1355 (2001)
15. L. Dal Negro, J.H. Yi, V. Nguyen, Y. Yi, J. Michel, L.C. Kimerling, Appl. Phys. Lett. **86**, 261905 (2005)
16. T.Y. Kim, N.M. Park, K.H. Kim, G.Y. Sunga, Y.W. Ok, T.Y. Seong, C.J. Choi, Appl. Phys. Lett. **85**, 5355 (2004)
17. T.V. Torchynska, J.L. Casas Espinola, E. Vergara Hernandez, L. Khomenkova, F. Delachat, A. Slaoui, Thin Solid Films **581**, 65 (2015)
18. T.V. Torchynska, J.L. Casas Espinola, L. Khomenkova, E. Vergara Hernandez, J.A. Andraca Adame, A. Slaoui, Mater. Sci. Semicond. Process. **37**, 46–50 (2015)
19. M. Wang, D. Li, Zh Yuan, D. Yang, D. Que, Appl. Phys. Lett. **90**, 131903 (2007)
20. J. Kistner, X. Chen, Y. Weng, H.P. Strunk, M.B. Schubert, J.H. Werner, J. Appl. Phys. **110**, 023520 (2011)
21. M. Molinari, H. Rinnert, M. Vergnat, J. Appl. Phys. **101**, 123532 (2007)
22. A. Rodriguez-Gómez, A. García-Valenzuela, E. Haro-Poniatowski, J.C. Alonso-Huitrón, J. Appl. Phys. **113**, 233102 (2013)
23. T.V. Torchynska, Y. Goldstein, A. Many, J. Jedrzejewskii, A.V. Kolobov, Microelectron. Eng. **66**, 83–90 (2003)
24. L. Khomenkova, F. Gourbilleau, J. Cardin, O. Jambois, B. Garrido, R. Rizk, J. Lumin. **129**, 1519 (2009)
25. S.V. Deshpande, E. Gulari, S.W. Brown, S.C. Rand, J. Appl. Phys. **77**, 6534–6541 (1995)
26. C.M. Mo, L.D. Zhang, C.Y. Xie, T. Wang, J. Appl. Phys. **73**, 5185 (1993)
27. W.I. Warren, P.M. Lenahan, S.E. Curry, Phys. Rev. Lett. **65**, 207 (1990)
28. B. Sain, D. Das, Phys. Chem. Chem. Phys. **15**, 3881 (2013)
29. H.L. Hsiao, A.B. Yang, H.L. Hwang, J. Phys. Chem. Sol. **69**, 278 (2008)
30. V. Alex, S. Finkbeiner, J. Weber, J. Appl. Phys. **79**, 6943 (1996)
31. C.H. Cho, B.H. Kim, T.W. Kim, S.J. Park, N.M. Park, G.Y. Sung, Appl. Phys. Lett. **86**, 143107 (2005)